Available online at www.medicinescience.org

ORIGINAL ARTICLE

Medicine Science International Medical Journal

Medicine Science 2026;15(2):796-805

Digital mammography lesion imaging features and breast cancer subtype

Ela Kaplan[1], Melahat Poyraz[2]

[1]Adıyaman University Faculty of Medicine, Department of Radiology, Adıyaman, Türkiye
[2]Elazığ Fethi Sekin City Hospital, Department of Radiology, Elazığ, Türkiye

Received 13 October 2025; Accepted 26 January 2026
Available online 22 May 2026 with doi: 10.5455/medscience.2025.10.279

Content of this journal is licensed under a Creative Commons Attribution-NonCommercial-NonDerivatives 4.0 International License.

Abstract

Breast cancer stands as one of the leading cancer types which causes numerous deaths throughout the world. Mammography serves as a standard tool for detecting breast cancer at its early stages of early development and diagnosis. The various molecular subtypes of breast cancer show different reactions to treatments and have different outcomes for patients. The research aims to establish the ability of visual lesion features in digital mammography images to identify breast cancer molecular subtypes. The research involved 194 patients who received breast cancer diagnoses through biopsy and their mammography results showed BI-RADS 4A, 4B, 4C or 5 lesions with breast density C and D. ER (estrogen receptor), PR (progesterone receptor), HER2 (human epidermal growth factor receptor 2), and Ki 67 values were obtained from pathology reports. The researchers studied breast cancer lesion characteristics through right/left breast positioning and upper/outer-lower/inner quadrant placement and they evaluated margin characteristics and lesion shape and dimensions and tumor size and microcalcification types and distribution patterns. The study found that microcalcification presence linked to both ER-positive (p=0.012) and PR-positive (p=0.038) breast cancer cases. The research found that younger patients with triple-negative breast cancer had tumors that exceeded 20 mm in size and round shapes. However, shape-based findings should be interpreted cautiously due to the limited number of round lesions. The presence of indistinct margins in breast cancer images were strongly associated with triple-negative breast cancer. Visual mammographic features are generally insufficient for accurate prediction of molecular subtypes, except for certain associations observed in triple-negative breast cancer. Future studies integrating radiomic analysis, artificial intelligence-based approaches, and larger cohorts are warranted.

Keywords: Breast cancer subtypes, mammography, molecular classification

Introduction

The most common malignant neoplasm in women is breast cancer (BCA) [1]. Early detection of BCA is important to reduce mortality [2]. Mammography is still the most widely used imaging modality for breast cancer screening. It has evolved tremendously from direct-exposure film mammography to xeromammography to screen-film mammography to the full-field digital mammography and finally the current era of digital breast tomosynthesis [3,4]. Despite the extensive transformation, the sensitivity of mammography is still limited by high breast density [5,6]. The overall sensitivity and specificity rate of mammography varies between 75-90% and 80-90% [5].

The heterogeneity of tumor morphology in BCA is due to different gene expression [7,8]. Classification of molecular subtypes of BCA is used as a precursor in planning of treatment, determining prognosis and assessment of treatment response [9]. Morphological variations in tumor structure and variability in the expression of different markers are stated as intratumoral heterogeneity [10,11]. Because of this entity, biopsy samples taken from the lesion may not always reflect the complete histopathological features of a lesion. Therefore, supplementing histopathological diagnosis using non-invasive imaging methods is much looked forward by clinicians [12,13].

Histopathology findings and typical features of tumoral lesions have been found to be reflected in radiological imaging features [14,15]. Predicting tumoral genotype from radiology images is a new promising field, called radio genomics [16,17]. The main benefits of radiogenomics are to determine the gene expression of the tumor by evaluating the whole tumoral lesion instead of small-sized biopsy materials taken from the tumors, to plan and evaluate the treatment response independent of tumoral size,

CITATION
Kaplan E, Poyraz M. Digital mammography lesion imaging features and breast cancer subtype. Med Science. 2026;15(2):796-805.

Corresponding Author: Ela Kaplan, Adıyaman University Faculty of Medicine, Department of Radiology, Adıyaman, Türkiye
Email: elakaplan15@gmail.com

DOI: 10.5455/medscience.2025.10.279

and to confirm the accuracy of clinical data by detecting gene abnormalities [16-18]. It is also not uncommon for a tumor to mutate and progress to a more aggressive and poorer prognosis subtype throughout treatment. The accurate identification of such situation is only possible with a repeat tissue biopsy, which then will determine the next level of treatment, or a change in treatment. Radiogenomic is a potential tool to assist these challenging circumstances.

The main objective of this study is to determine the effectiveness of distinguishing breast cancer subtypes using imaging features of lesions in mammography images. This study focuses exclusively on visually assessed, conventional mammographic features as defined by the Breast Imaging Reporting and Data System (BI-RADS) lexicon.

Material and Methods

Study Population and Sample

Our study was designed as a retrospective cross-sectional study. Initially, 7928 patients who underwent mammography between 2017 and 2021 were screened. Patients with benign pathology, inconclusive biopsy results, or unavailable imaging data were excluded resulting in a final study population of 194 patients. The ACR BI-RADS classification was used as the basis for determining the inclusion criteria. Patients with breast density C (heterogeneous fibroglandular tissue) or D (dense fibroglandular tissue), who had a lesion detected in mammography in the BI-RADS 4A, 4B, 4C or 5 category, and whose breast cancer diagnosis was subsequently confirmed by core needle biopsy under ultrasound guidance, were included in the study [19,20]. Patients with inconclusive biopsy results, those with benign pathology, or those for whom imaging data were unavailable were excluded from the study. The number of patients included in the study was consistent with the sample sizes reported in similar radiogenomic studies in the literature (range 91-216 patients) [21,22]. Mammographic findings were evaluated according to the ACR BI-RADS lexicon standard, while molecular subtypes were defined according to the WHO 2019 classification [23] (Figure 1, Figure 2).

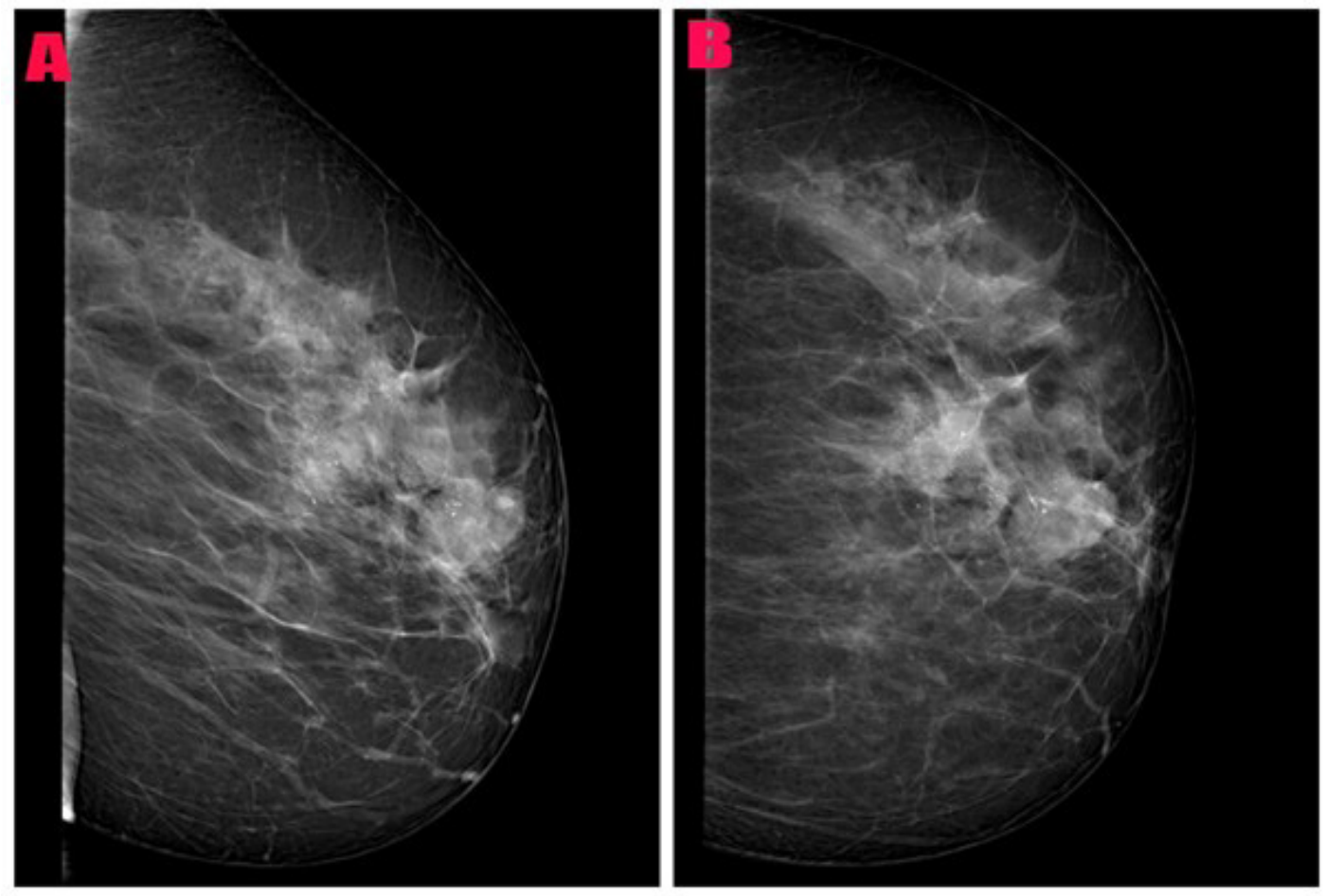

Figure 1. Representative example of mammographic features of HER2-positive breast cancer. (A) Left MLO view; (B) Left CC view showing retroareolar ill-defined opacity with clustered pleomorphic calcifications in segmental distribution. MLO: mediolateral oblique; CC: craniocaudal

DOI: 10.5455/medscience.2025.10.279

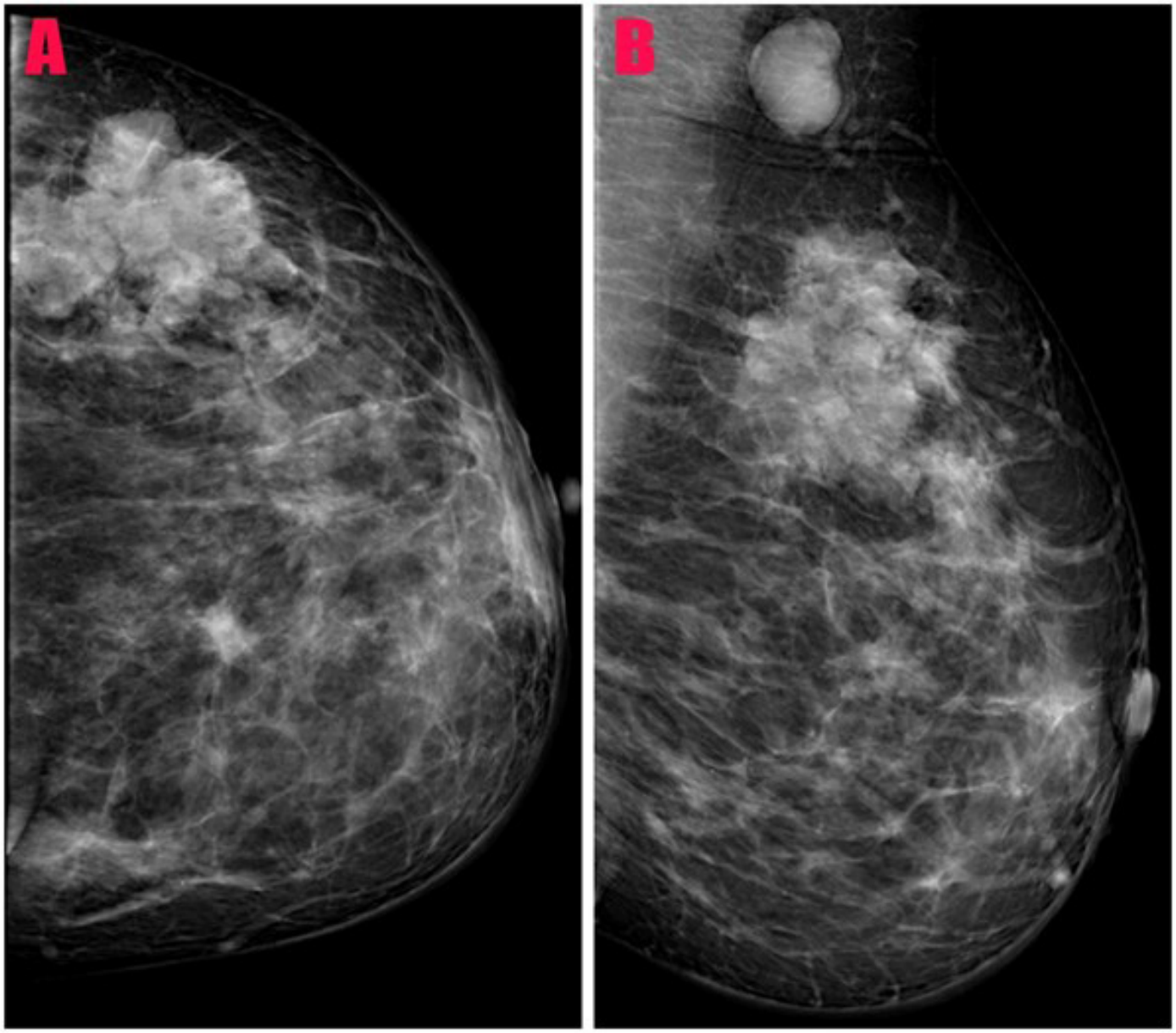

Figure 2. Representative example of hormone receptor-positive breast cancer mammography. (A) Left CC view showing irregular high-density mass in upper outer quadrant; (B) Left MLO view demonstrating the mass measuring 52×42 mm with microlobulated margins, associated skin thickening and axillary lymphadenopathy. Histopathology: ER-positive, PR-positive, HER2-negative invasive carcinoma. CC: craniocaudal; MLO: mediolateral oblique; ER: estrogen receptor; PR: progesterone receptor; HER2: human epidermal growth factor receptor 2

Study Procedures

Patients' mammography images were obtained digitally from the hospital radiology archive. All mammographic examinations were performed using a full-field digital mammography system in standard mediolateral oblique and craniocaudal projections. For each patient, the location of the lesion (right or left breast; upper outer, lower outer, upper inner, lower inner, or upper central quadrant), morphological characteristics (oval, round or irregular shape), edge characteristics (spiculated, limited, microlobulated, indistinct or blurred contour) and dimensions in millimetres for the long and short axes were recorded. Where microcalcifications were present, these were classified as amorphous, fine pleomorphic, fine linear branching or coarse heterogeneous, and their distribution patterns (segmental, grouped/clustered, regional, linear, or diffuse) were documented [21,20]. The images were evaluated by consensus between two radiologists specialising in breast radiology with at least ten years of experience. Information on oestrogen receptor, progesterone receptor, HER2 status and Ki-67 proliferation index was obtained from pathology reports [19].

DOI: 10.5455/medscience.2025.10.279

Identification of Molecular Subtypes

The molecular classification of invasive breast carcinomas was performed according to the 2019 WHO criteria. Estrogen receptor (ER) and progesterone receptor (PR) status were evaluated as part of molecular classification. The Luminal A-like subtype was defined as tumours that were ER positive, PR positive, HER2 negative, and had a Ki-67 index below 15% [21,22]. The Luminal B-like group was divided into two categories. HER2 negative tumours comprised cases that were ER positive, HER2 negative, and either PR negative or weakly positive, or had a Ki-67 index above 30%. HER2 positive tumours included tumours that were ER positive and HER2 overexpressed or amplified, regardless of PR and Ki-67 values. The HER2 positive subtype included carcinomas that were ER and PR negative with HER2 overexpression or amplification. The triple-negative group consisted of cases that were negative for all three receptors (ER, PR, and HER2) [21-25].

Statistical Analysis

Data were analysed using the SPSS 22.0 software package (International Business Machines Corp., Armonk, NY, USA). The normality of the variables was assessed using the Shapiro-Wilks test. Continuous variables were expressed as mean and standard deviation, while categorical variables were expressed as number and percentage. The relationship between microcalcification types and ER and PR status was examined using the chi-square test. When the proportion of cells with an expected value less than five exceeded twenty percent, Fisher's exact test was applied. Multinomial logistic regression analysis was performed to evaluate the success of mammographic features in predicting breast cancer subtypes. In this analysis, the Luminal A subtype was designated as the reference category, and age, lesion shape, tumor size, margin characteristics, microcalcification type, microcalcification distribution, and lesion location were included in the model as independent variables. All tests were performed bilaterally, and results with a p-value below 0.05 were considered statistically significant.

Ethical Considerations

The research protocol was reviewed by the Non-Invasive Clinical Research Ethics Committee of Adıyaman University hospital's Faculty of Medicine and approved with decision number 2021/08-13 dated 26 October 2021. All stages of the study were conducted in accordance with the principles of the Declaration of Helsinki. Due to the retrospective design, informed consent from patients was not required. To protect patient confidentiality, all personal data were coded and anonymised, and analyses were performed in this manner.

Results

Study Population Characteristics

The research included 194 female breast cancer patients who had an average age of 42.22 years with a standard deviation of 11.25 years. The research included 194 female breast cancer patients with a mean age of 42.22 ± 11.25 years. Breast tissue composition showed BI-RADS type C (heterogeneously dense) breasts in 52.6% of cases and BI-RADS type D (extremely dense) breasts in 47.4%. The young age of our study participants explains why dense breast tissue continues to be prevalent in this population (Table 1).

Table 1. Demographic, clinical, and digital mammographic radiological characteristics of the study population

Characteristic		n (%) / Mean ± SD
Age (mean ± SD)		42.22 ± 11.25
Breast density	**C (Heterogeneous fibroglandular tissue)**	102 (52.6)
	D (Dense fibroglandular tissue)	92 (47.4)
Lesion shape	**Irregular**	188 (96.9)
	Oval	0 (0.0)
	Round	6 (3.1)
Lesion measurements (mm, mean ± SD)	**Long axis**	28.26 ± 15.08
	Short axis	18.74 ± 10.51
Lesion margins	**Spiculated**	132 (68.0)
	Well-circumscribed	6 (3.1)
	Indistinct	11 (5.7)
	Microlobulated	39 (20.1)
	Obscured	6 (3.1)
Microcalcification	**None**	86 (44.3)
	Amorphous	44 (22.7)
	Fine pleomorphic	45 (23.2)
	Fine linear branching	13 (6.7)
	Coarse heterogeneous	6 (3.1)
Microcalcification distribution (n=108)*	**Segmental**	31 (28.7)
	Grouped/Clustered	42 (38.9)
	Regional	18 (16.7)
	Linear	11 (10.2)
	Diffuse	6 (5.5)
Lesion location (right/left)	**Right**	96 (49.5)
	Left	98 (50.5)
Quadrant location	**Upper outer quadrant**	117 (60.3)
	Lower outer quadrant	9 (4.6)
	Upper inner quadrant	32 (16.5)
	Lower inner quadrant	19 (9.8)
	Upper central quadrant	17 (8.8)

*Only for cases with microcalcifications

Mammographic Findings and Lesion Characteristics

The mammographic evaluation showed specific patterns in how lesions appeared. The majority of tumors showed irregular

DOI: 10.5455/medscience.2025.10.279

shapes at 96.9% while only 3.1% had round shapes and no lesions matched the oval category which was part of the initial assessment criteria. The tumors measured an average of 28 millimeters in length and 19 millimeters in width. The tumor sizes indicated that most lesions were found at an intermediate stage between early and advanced stages (Table 1). The tumor size distribution showed that 118 patients (60.8%) had tumors measuring 20mm or larger while 76 patients (39.2%) had tumors smaller than 20mm.

The majority of lesions presented with spiculated edges which made up about two-thirds of all cases. The second most common margin pattern was microlobulated while well-circumscribed and indistinct and obscured margins appeared rarely. The high frequency of spiculated margins in this study matches the typical appearance of malignant tumors during mammography (Table 1).

The analysis showed that microcalcifications were absent in approximately half of the examined cases. The two most common calcification patterns in patients with calcifications were amorphous and fine pleomorphic which each affected about 25% of the patients. The occurrence of fine linear branching and coarse heterogeneous calcifications was relatively rare. The 108 cases with microcalcifications showed grouped/clustered distribution as the most common pattern at 38.9% followed by segmental at 28.7% and regional at 16.7% and linear at 10.2% and diffuse at 5.5%. The lesions demonstrated no preference for breast side since they occurred with equal frequency in both breasts. The majority of tumors developed in the upper outer quadrant of the breast which matches the distribution of breast tissue volume (Table 1).

Molecular Subtypes and Histological Classification

The molecular analysis of tumors showed Luminal A as the leading subtype which made up more than one-third of all cases. The second largest group consisted of Luminal B HER2-positive tumors followed by Luminal B HER2-negative tumors. The HER2-positive and triple-negative subtypes made up less patterns but the low number of triple-negative cases stands out (Table 2).

Table 2. Breast cancer characteristics in the selected patient dataset

Characteristic		n (%)
Molecular subtypes of breast cancer	Luminal A	72 (37.1)
	Luminal B HER2-	40 (20.6)
	Luminal B HER2+	54 (27.8)
	HER2+	18 (9.3)
	Triple-negative	10 (5.2)
Histological type of breast cancer	Invasive ductal carcinoma	182 (93.8)
	Invasive lobular carcinoma	12 (6.2)

Note: n: number; ER: Estrogen receptor; PR: Progesterone receptor; HER2: Human epidermal growth factor receptor 2

Invasive ductal carcinoma accounted for more than 90% of all cases, while invasive lobular carcinoma represented a small minority (Table 2).

Association Between Molecular Subtypes and Imaging Features

The multinomial logistic regression analysis investigated how tumor subtypes relate to mammographic features through Luminal A as the reference group. The analysis used spiculated margins as the reference point for all margin assessments because this presentation occurred most frequently in 68% of cases. The statistical power for shape comparisons remained restricted because the study included only six round lesions and no oval lesions.

The research found that younger women had increased chances of developing triple-negative breast cancer according to age-related data (OR=0.937, p=0.049). The analysis revealed tumor size as a critical factor for triple-negative breast cancer diagnosis because tumors larger than 20mm had 2.67 times higher odds than smaller tumors (OR=2.670, p=0.038). The study found that triple-negative cancers had a higher probability of being round in shape compared to Luminal A tumors although the number of round lesions remained small (OR=7.170, p=0.045). The study results indicated that HER2-positive tumors tended to grow larger (OR=2.130, p=0.072).

Most tumor subtypes showed minimal distinction when their margins were evaluated against the spiculated reference category. The analysis showed that indistinct margins tended to link with Luminal B HER2-negative tumors (OR=5.108, p=0.097) and strongly linked with triple-negative cancers (OR=8.953, p=0.035) because of their aggressive tumor behavior. The analysis of well-circumscribed margin category remained unreliable because of insufficient data.

The analysis of different microcalcification patterns against the absence of calcifications failed to produce any statistically significant results for molecular subtype identification. The distribution pattern of segmental calcifications demonstrated a possible link with HER2-positive tumors (OR=3.367, p=0.089) but other distribution patterns failed to show meaningful connections with particular molecular subtypes (Table 3).

Hormone Receptor Status and Microcalcification Patterns

The analysis between hormone receptor expression and microcalcification patterns produced interesting results. The absence of calcifications occurred more often in tumors that lacked progesterone receptor expression than in tumors that expressed progesterone receptors. The presence of both amorphous and fine pleomorphic calcifications was more common in tumors that were PR-positive. The imaging results showed that PR-negative tumors presented with fine linear branching patterns more often than PR-positive tumors. The results demonstrated that PR status affects the development of calcifications because they reached statistical significance (Table 4).

DOI: 10.5455/medscience.2025.10.279

Table 3. Distribution of variables in terms of survivor and deceased patients

Subtype / Variable		β	p-value	OR	95% CI Lower	95% CI Upper
Luminal B HER2+						
Age		0.015	0.428	1.015	0.978	1.054
Tumor size ≥20mm (ref: <20mm)		0.421	0.186	1.523	0.819	2.833
Shape - Round (ref: Irregular)†		-1.085	0.051	0.338	0.114	1.003
Margin (ref: Spiculated)	**Well-circumscribed**	*	*	*	*	*
	Indistinct	0.502	0.697	1.653	0.431	6.341
	Microlobulated	-0.851	0.353	0.427	0.171	1.066
	Obscured	-0.777	0.636	0.460	0.118	1.792
Microcalcification (ref: None)	**Amorphous**	-0.833	0.443	0.435	0.152	1.245
	Fine pleomorphic	-0.294	0.785	0.746	0.291	1.913
	Fine linear branching	-1.011	0.417	0.364	0.132	1.004
	Coarse heterogeneous	*	*	*	*	*
Calcification distribution - Segmental‡		0.892	0.124	2.441	0.786	7.582
Location - Upper outer quadrant		0.214	0.766	1.239	0.301	5.094
Luminal B HER2-						
Age		-0.015	0.526	0.985	0.939	1.033
Tumor size ≥20mm (ref: <20mm)		0.287	0.412	1.332	0.672	2.641
Shape - Round (ref: Irregular)†		-0.591	0.693	0.554	0.129	2.378
Margin (ref: Spiculated)	**Well-circumscribed**	*	*	*	*	*
	Indistinct	1.631	0.097	5.108	0.918	28.433
	Microlobulated	-1.426	0.298	0.240	0.016	3.514
	Obscured	0.113	0.874	1.120	0.275	4.558
Microcalcification (ref: None)	**Amorphous**	0.228	0.892	1.256	0.347	4.547
	Fine pleomorphic	0.793	0.433	2.210	0.685	7.131
Calcification distribution - Segmental‡		0.645	0.318	1.906	0.542	6.704
Location - Upper outer quadrant		1.642	0.151	5.164	0.550	48.522
HER2+						
Age		0.005	0.881	1.005	0.945	1.068
Tumor size ≥20mm (ref: <20mm)		0.756	0.072	2.130	0.934	4.857
Shape - Round (ref: Irregular)†		1.264	0.216	3.539	0.493	25.411
Margin (ref: Spiculated)	**Microlobulated**	0.830	0.391	2.292	0.639	8.226
	Obscured	-0.705	0.410	0.494	0.092	2.648
Microcalcification (ref: None)	**Amorphous**	1.010	0.297	2.746	0.612	12.316
	Fine pleomorphic	1.350	0.147	3.857	0.821	18.127
Calcification distribution - Segmental‡		1.214	0.089	3.367	0.835	13.574
Location - Upper outer quadrant		-0.171	0.864	0.843	0.119	5.956
Triple-Negative						
Age		-0.065	0.049	0.937	0.879	0.999
Tumor size ≥20mm (ref: <20mm)		0.982	0.038	2.670	1.056	6.748
Shape - Round (ref: Irregular)†		1.970	0.045	7.170	1.042	49.333
Margin (ref: Spiculated)	**Indistinct**	2.192	0.035	8.953	1.173	68.342
	Obscured	1.761	0.090	5.819	0.750	45.132
Microcalcification (ref: None)	**Amorphous**	1.286	0.196	3.618	0.528	24.788
	Fine pleomorphic	1.007	0.299	2.737	0.412	18.187
Calcification distribution - Segmental‡		-0.543	0.624	0.581	0.065	5.193
Location - Upper outer quadrant		-0.331	0.824	0.718	0.039	13.180

Notes: Model fit statistics: -2 Log Likelihood = 418.32, Nagelkerke R^2 = 0.312. †Oval lesions were not observed in the study population (n=0). ‡Only for cases with microcalcifications (n=108). *Not estimable due to small sample size or model convergence issues. Only variables with p<0.10 or clinical significance are shown for some categories

DOI: 10.5455/medscience.2025.10.279

Table 4. Comparison of microcalcification presence according to ER and PR status and distribution of molecular subtypes (n = 194)

Calcification type	PR negative n (%)	PR positive n (%)	Total n (%)	ER negative n (%)	ER positive n (%)	Total n (%)
None	22 (55.0)	64 (41.0)	86 (44.3)	23 (67.6)	63 (39.4)	86 (44.3)
Fine pleomorphic	6 (15.0)	39 (25.0)	45 (23.2)	4 (11.8)	41 (25.6)	45 (23.2)
Amorphous	4 (10.0)	40 (25.6)	44 (22.7)	3 (8.8)	41 (25.6)	44 (22.7)
Fine linear branching	6 (15.0)	7 (4.5)	13 (6.7)	4 (11.8)	9 (5.6)	13 (6.7)
Coarse heterogeneous	2 (5.0)	4 (2.6)	6 (3.1)	0 (0.0)	6 (3.8)	6 (3.1)
Total	40 (100)	154 (100)	194 (100)	28 (100)	166 (100)	194 (100)

Statistical comparison: PR status ($\chi^2 = 10.142$, p = 0.038); ER status ($\chi^2 = 12.846$, p = 0.012)

The relationship between ER status and mammographic calcification patterns proved to be more pronounced than other factors. The majority of tumors without estrogen receptors (ER-negative) did not contain calcifications since more than two-thirds of these tumors showed no calcification. The calcification patterns of ER-positive tumors showed diversity because amorphous and fine pleomorphic calcifications appeared in similar proportions among these cases. The absence of coarse heterogeneous calcifications in ER-negative tumors compared to their presence in ER-positive tumors demonstrated the distinct patterns between these groups. The results demonstrated that ER status plays a major role in determining mammographic calcification patterns because they reached statistical significance (Table 4).

Integration of Molecular and Hormonal Profiles

The molecular subtypes matched their hormone receptor status according to established biological principles. The molecular definition of Luminal A tumors was fully supported by the presence of both estrogen and progesterone receptors in all cases. The Luminal B HER2-negative tumors maintained ER-positive status but displayed PR-negative results in some cases which matches the known diversity of this subtype. All Luminal B HER2-positive tumors displayed ER expression and most of them also showed PR expression. The molecular classification of HER2-positive and triple-negative tumors was confirmed by their complete absence of hormone receptors (Table 5).

Table 5. Distribution of molecular subtypes and hormone receptor status

Molecular subtype	n	ER status	PR status
Luminal A	72	Positive (72)	Positive (72)
Luminal B HER2-	40	Positive (40)	Positive (32) / Negative (8)
Luminal B HER2+	54	Positive (54)	Positive (50) / Negative (4)
HER2+	18	Negative (18)	Negative (18)
Triple negative	10	Negative (10)	Negative (10)
Total	194	ER+: 166 / ER-: 28	PR+: 154 / PR-: 40

Note: ER: Estrogen receptor; PR: Progesterone receptor; HER2: Human epidermal growth factor receptor 2

The detailed hormone receptor analysis supported the biological accuracy of molecular subtyping and demonstrated the expected diversity of Luminal B tumors which can have different progesterone receptor expression levels while maintaining estrogen receptor positivity. The testing method produced reliable results because triple-negative tumors were correctly identified through their complete absence of hormone receptors (Table 5).

Discussion

This study investigated the value of visually assessed mammographic features in distinguishing molecular subtypes of breast cancer using a retrospective patient cohort. Overall, the multinomial logistic regression analysis demonstrated that conventional mammographic parameters have limited ability to reliably predict molecular subtypes. Nevertheless, certain imaging and clinical characteristics showed subtype-specific associations. In particular, microcalcification presence was related to hormone receptor status, while age and lesion morphology appeared to be more informative for the triple-negative subtype. These findings suggest that although mammography provides restricted information for molecular subtype discrimination, it may still offer supportive insights in selected clinical contexts.

In the present study, the presence of mammographic microcalcifications was more frequently observed in hormone receptor-positive breast cancers. Overall, tumors expressing estrogen and progesterone receptors tended to demonstrate microcalcifications more often than hormone receptor-negative tumors. Previous studies have reported inconsistent findings

DOI: 10.5455/medscience.2025.10.279

regarding the relationship between hormone receptor status and calcification characteristics. While Wang et al. described an association between casting-type calcifications and estrogen and progesterone receptor negativity [21], Li et al. demonstrated that hormone receptor-positive/HER2-negative tumors with seemingly benign calcifications may be associated with activation of estrogen-related molecular pathways [26]. In addition, Luo et al. emphasized that the clinical implications of mammographic microcalcifications may vary according to molecular subtype, without specifically addressing estrogen and progesterone receptor status [20]. Differences in study populations, calcification classification methods, and imaging techniques may partly explain these discrepancies. Taken together, these findings suggest that microcalcification characteristics alone are insufficient for molecular subtype discrimination but may reflect underlying tumor biology in selected subgroups.

In the present study, although the Luminal A subtype constituted the largest proportion of cases, conventional mammographic features were generally insufficient to reliably distinguish breast cancer molecular subtypes. Multinomial logistic regression analysis demonstrated that most mammographic parameters lacked significant predictive value, with the exception of the triple-negative subtype. This observation is partially consistent with previous literature. Horvath reported that mammographic features do not provide definitive pathognomonic findings for molecular subtype differentiation [27]. Similarly, Davey et al., in their systematic review, concluded that conventional mammographic features show limited success in subtype discrimination, while more promising results have been reported for the triple-negative subtype [28]. Radiomic-based analyses have further supported the limited performance of traditional mammographic features for HER2-positive and luminal subtypes [29].

With respect to the triple-negative subtype, certain clinical and imaging characteristics appeared to be more informative. Consistent with prior reports, triple-negative tumors in our cohort tended to present in younger patients and with larger lesion sizes, and lesion morphology showed subtype-specific variation [29]. In contrast, mammographic features demonstrated minimal discriminatory value for other molecular subtypes, with only weak trends observed for selected parameters. Overall, these findings indicate that mammography has a limited role in molecular subtype determination, particularly outside the context of triple-negative breast cancer.

In the present study, although spiculated margins represented the most common mammographic finding, their association with molecular subtypes appeared to be complex. Previous studies have reported that spiculated margins are more frequently associated with luminal breast cancer profiles, particularly in ultrasound and contrast-enhanced mammography-based evaluations [30,31]. In contrast, our findings suggested that indistinct margins, rather than spiculated margins, were more commonly observed in triple-negative tumors.

This observation is in line with prior reports indicating that triple-negative breast cancers may present with less typical malignant imaging features and may lack classical spiculated margins [32]. The presence of indistinct margins also showed a tendency in the luminal B HER2 negative subtype, suggesting that margin characteristics may overlap among aggressive tumor subtypes. Although some studies have associated spiculated or angular margins with poorer prognosis in triple-negative breast cancer [33], our results indicate that aggressive molecular subtypes may demonstrate variable and sometimes atypical morphological patterns on mammography. Therefore, margin characteristics alone should be interpreted cautiously and within the broader clinical and biological context.

In the present study, microcalcification distribution patterns were also evaluated in relation to molecular subtypes. Although segmental distribution appeared more frequently in HER2-positive tumors, most distribution patterns showed limited discriminatory value for molecular subtype differentiation. The most common distribution pattern was grouped or clustered calcifications; however, this pattern did not demonstrate a specific association with any molecular subtype.

Previous studies have reported inconsistent findings regarding the relationship between microcalcification distribution patterns and molecular characteristics of breast cancer. Luo et al. demonstrated that HER2 positive tumors with microcalcifications may achieve better pathological complete response rates following neoadjuvant therapy, suggesting potential biological relevance beyond subtype identification [20]. In contrast, Wang et al. reported that cast-type calcifications are more commonly observed in tumors lacking estrogen and progesterone receptor expression [21]. Additionally, Li et al. showed that hormone receptor-positive/HER2 negative tumors with apparently benign calcifications may exhibit activation of estrogen-related molecular pathways [26].

Taken together, these findings suggest that microcalcification distribution patterns alone may not provide sufficient information for reliable molecular subtype prediction. Instead, the specific type of microcalcification, such as amorphous, pleomorphic, or cast-type patterns, may carry greater biological and clinical relevance than distribution patterns alone.

With respect to patient age, our findings indicate that age-related associations were primarily observed in the triple-negative subtype. Triple-negative breast cancer tended to occur in younger patients and was more frequently associated with larger tumor size at presentation, consistent with its known aggressive biological behavior. In contrast, age did not demonstrate a meaningful association with other molecular subtypes in our cohort.

Previous studies have reported variable results regarding the relationship between age and triple-negative breast cancer. While Wang et al. investigated reproductive risk factors in younger women without directly examining age-related subtype risk [21], Du and Li reported a higher incidence of triple-negative breast

cancer among women aged 20–44 years, particularly within specific ethnic populations [24]. Similarly, McCarthy et al. emphasized the strong association between triple-negative breast cancer and ethnic background, suggesting that the independent contribution of age may be difficult to isolate [22]. Howard and Olopade further highlighted the complex interplay between genetic, ethnic, and demographic factors in triple-negative breast cancer [25]. Taken together, these findings suggest that younger age may represent a supportive clinical indicator for triple-negative breast cancer, although its effect should be interpreted within a broader biological and demographic context.

This study has several limitations. First, its retrospective single-center design and relatively small sample size may limit the generalizability of the findings. In addition, a number of patients were excluded due to unavailable or incomplete archival imaging data, which may have introduced selection bias.

Despite these limitations, the study has notable strengths, including image evaluation performed by experienced breast radiologists who reached consensus and the use of a standardized molecular classification system based on the World Health Organization criteria. Nevertheless, further research involving larger, multicenter cohorts is required to better define the role of mammography in molecular subtype determination. Future studies integrating radiomic analysis and artificial intelligence-based image processing techniques may improve diagnostic performance by capturing quantitative imaging features beyond visual assessment.

Conclusion

Screening mammography remains the primary and most effective imaging modality for the early detection of breast cancer. However, previous studies have reported inconsistent results regarding the ability of mammographic features to reliably identify breast cancer molecular subtypes. In the present study, visually assessed conventional mammographic features alone were generally insufficient for accurate molecular subtype prediction.

Nevertheless, certain clinical and imaging characteristics appeared to be more informative for the triple-negative subtype, suggesting that mammography may provide supportive, but not definitive, information in selected clinical contexts. Overall, these findings highlight the limited role of conventional mammography in molecular subtype determination. Further studies incorporating quantitative radiomic analysis, artificial intelligence-based approaches, and larger, more diverse patient populations are required to improve the accuracy and clinical utility of non-invasive molecular subtype identification.

Ethical Approval
Approved by the Institutional Ethics Committee of Adıyaman University Ethics Committee (No: 2021/08-13, Date: 26 October 2021).

Patient Consent
Informed consent was waived due to the retrospective design.

Conflict of Interest
The authors declare no conflict of interest.

Funding
The authors received no financial support for this study.

References

1. Marmot MG, Altman DG, Cameron DA, et al. The benefits and harms of breast cancer screening: an independent review. Br J Cancer. 2013;108:2205-40.
2. Li X, Qin G, He Q, et al. Digital breast tomosynthesis versus digital mammography: integration of image modalities enhances deep learning-based breast mass classification. Eur Radiol. 2020;30:778-88.
3. Ma W, Zhao Y, Ji Y, et al. Breast cancer molecular subtype prediction by mammographic radiomic features. Acad Radiol. 2019;26:196-201.
4. Joe BN, Sickles EA. The evolution of breast imaging: past to present. Radiology. 2014;273:S23-44.
5. Conti A, Duggento A, Indovina I, Guerrisi M, Toschi N. Radiomics in breast cancer classification and prediction. Semin Cancer Biol. 2021;72:238-50.
6. Hogg P, Kelly J, Mercer C, eds. Digital mammography: a holistic approach. Cham: Springer; 2015.
7. Apanovich N, Shubin V, Korotaeva A, et al. Molecular genetic markers of breast cancer. Tumors Female Reprod Syst. 2014;1:19-28.
8. Wu M, Ma J. Association between imaging characteristics and different molecular subtypes of breast cancer. Acad Radiol. 2017;24:426-34.
9. Senkus E, Kyriakides S, Ohno S, et al. Primary breast cancer: ESMO clinical practice guidelines for diagnosis, treatment and follow-up. Ann Oncol. 2015;26:v8-30.
10. Turashvili G, Brogi E. Tumor heterogeneity in breast cancer. Front Med (Lausanne). 2017;4:227.
11. Gerashchenko TS, Denisov EV, Litviakov NV, et al. Intratumor heterogeneity: nature and biological significance. Biochemistry (Mosc). 2013;78:1201-15.
12. Januškevičienė I, Petrikaitė V. Heterogeneity of breast cancer: the importance of interaction between different tumor cell populations. Life Sci. 2019;239:117009.
13. Lin F, Wang Z, Zhang K, et al. Contrast-enhanced spectral mammography-based radiomics nomogram for identifying benign and malignant breast lesions of sub-1 cm. Front Oncol. 2020;10:573630.
14. Gillies RJ, Kinahan PE, Hricak H. Radiomics: images are more than pictures, they are data. Radiology. 2016;278:563-77.
15. Lambin P, Leijenaar RTH, Deist TM, et al. Radiomics: the bridge between medical imaging and personalized medicine. Nat Rev Clin Oncol. 2017;14:749-62.
16. Porcu M, Solinas C, Mannelli L, et al. Radiomics and "radiomics" in cancer immunotherapy: a guide for clinicians. Crit Rev Oncol Hematol. 2020;154:103068.
17. Ognerubov N, Shatov I, Shatov A. Radiogenomics and radiomics in the diagnostics of malignant tumours: a literary review. Vestn Tambov Univ. 2017;22:1453-60.
18. Pesapane F, Suter MB, Rotili A, et al. Will traditional biopsy be substituted by radiomics and liquid biopsy for breast cancer diagnosis and characterisation?. Med Oncol. 2020;37:29.

19. Peng H, Zhu Y, Li Y. Correlation analysis of ultrasound features with ER, PR, HER-2, P53, Ki-67, TOPIIa, and CK5/6 in non-mass infiltrating ductal carcinoma. Ginekol Pol. 2025.

20. Luo Z, Hu J, Kong D, et al. Mammographic microcalcifications as a predictor of neoadjuvant efficacy across different breast cancer molecular subtypes. Asian J Surg. 2025;48:2902-10.

21. Wang J, Zhao L, Hu X, et al. Clinicopathological characteristics and prognostic significance of casting-type calcifications in invasive breast cancer. Sci Rep. 2024;14:13351.

22. McCarthy AM, Friebel-Klingner T, Ehsan S, et al. Relationship of established risk factors with breast cancer subtypes. Cancer Med. 2021;10:6456-67.

23. Tan PH, Ellis I, Allison K, et al. The 2019 WHO classification of tumours of the breast. Histopathology. 2020;77:181-85.

24. Du XL, Li Z. Incidence trends in triple-negative breast cancer among women in the United States. Am J Cancer Res. 2023;13:678-91.

25. Howard FM, Olopade OI. Epidemiology of triple-negative breast cancer: a review. Cancer J. 2021;27:8-16.

26. Li Y, Xu Y, Lin C, et al. Calcification-associated molecular traits and therapeutic strategies in HR+/HER2− breast cancer. Cancer Biol Med. 2024;21:400-15.

27. Horvath E. Molecular subtypes of breast cancer—what breast imaging radiologists need to know. Rev Chil Radiol. 2021;27:17-26.

28. Davey MG, Davey MS, Boland MR, et al. Radiomic differentiation of breast cancer molecular subtypes using pre-operative imaging: a systematic review and meta-analysis. Eur J Radiol. 2021;144:109996.

29. Son J, Lee SE, Kim EK, Kim S. Prediction of breast cancer molecular subtypes using radiomics signatures of synthetic mammography. Sci Rep. 2020;10:21566.

30. Ramírez-Galván Y, Uribe-Martínez M, Ponce-Camacho M, Montemayor-Martínez A. Spiculated margin on ultrasound is associated with tumor grade and immunohistochemical profile in breast cancer. J Mex Fed Radiol Imaging. 2022;1:119-25.

31. Li N, Gong W, Xie Y, Sheng L. Correlation between CEM imaging characteristics and molecular subtypes of breast cancer. Breast. 2023;72:103595.

32. Schopp JG, Polat DS, Arjmandi F, et al. Imaging challenges in diagnosing triple-negative breast cancer. Radiographics. 2023;43:e230027.

33. Sheng D, Shen X, Shi Z, et al. Survival outcome assessment for triple-negative breast cancer: a nomogram analysis. Eur Radiol. 2022;32:6575-87.